Editors' Suggestion | Featured in Physics

Measurement of *CP*-Averaged Observables in the $B^0 \to K^{*0}\mu^+\mu^-$ Decay

R. Aaij *et al.*[*]
(LHCb Collaboration)

(Received 11 March 2020; accepted 28 May 2020; published 2 July 2020)

An angular analysis of the $B^0 \to K^{*0}(\to K^+\pi^-)\mu^+\mu^-$ decay is presented using a dataset corresponding to an integrated luminosity of 4.7 fb^{-1} of pp collision data collected with the LHCb experiment. The full set of *CP*-averaged observables are determined in bins of the invariant mass squared of the dimuon system. Contamination from decays with the $K^+\pi^-$ system in an *S*-wave configuration is taken into account. The tension seen between the previous LHCb results and the standard model predictions persists with the new data. The precise value of the significance of this tension depends on the choice of theory nuisance parameters.

DOI: 10.1103/PhysRevLett.125.011802

Decays mediated by the quark-level transition $b \to s\ell^+\ell^-$, where ℓ represents a lepton, have been the subject of intense recent study, as angular observables [1–8], branching fractions [8–11], and ratios of branching fractions between decays with different flavors of leptons [12–16] have been measured to be in tension with standard model (SM) predictions. Such decays are suppressed in the SM, as they proceed only through amplitudes that involve electroweak loop diagrams. The decays are sensitive to virtual contributions from new particles, which could have masses that are inaccessible to direct searches. The observed anomalies with respect to SM predictions can be explained consistently in new physics models that introduce an additional vector or axial-vector contribution [17–35]. However, there is still considerable debate about whether some of the observations might instead be explained by hadronic uncertainties associated with the transition form factors, or by other long-distance effects [36–39].

The LHCb Collaboration presented a measurement of the angular observables of the $B^0 \to K^{*0}\mu^+\mu^-$ decay in Ref. [1] and found that the data could be explained by modifying the real part of the vector coupling strength of the decays, conventionally denoted $\mathcal{R}e(C_9)$. The analysis used the nuisance parameters from Ref. [40], implemented in the EOS software package described in Ref. [41], and found a 3.4 standard deviation (σ) tension with the SM value of $\mathcal{R}e(C_9)$. The tension observed depends on the values of various SM nuisance parameters, including form-factor parameters and subleading corrections used to account for long-distance QCD interference effects with the charmonium modes. Using the FLAVIO software package [42], with its default SM nuisance parameters, gives a tension of 3.0σ with respect to the SM value of $\mathcal{R}e(C_9)$ when fitting the angular observables from Ref. [1]. The nuisance parameters include a recent treatment of the subleading corrections [43,44] that was not available at the time of the previous analysis.

This Letter presents the most precise measurements of the complete set of *CP*-averaged angular observables in the decay $B^0 \to K^{*0}\mu^+\mu^-$. The dataset corresponds to an integrated luminosity of 4.7 fb^{-1} of pp collisions collected with the LHCb experiment. The data were taken in the years 2011, 2012, and 2016, at center-of-mass energies of 7, 8, and 13 TeV, respectively. The analysis uses the same technique as the analysis described in Ref. [1] but the data sample contains approximately twice as many B^0 decays, owing to the addition of the 2016 data. The $b\bar{b}$ production cross section increases by roughly a factor of 2 between the Run 1 and 2016 datasets [45]. The same 2011 and 2012 (Run 1) data as in Ref. [1] are used in the present analysis. The results presented in this Letter supersede the previous LHCb publication. The combination of the Run 1 dataset with the 2016 dataset requires a simultaneous angular fit to account for efficiency and reconstruction differences between years. Throughout this Letter, K^{*0} is used to refer to the $K^*(892)^0$ resonance and the inclusion of charge-conjugate processes is implied. The K^{*0} meson is reconstructed through the decay $K^{*0} \to K^+\pi^-$.

The final state of the $B^0 \to K^{*0}\mu^+\mu^-$ decay can be described by the invariant mass squared of the dimuon system q^2, the invariant mass of the $K^+\pi^-$ system, and the three decay angles, $\vec{\Omega} = (\cos\theta_l, \cos\theta_K, \phi)$. The angle between the μ^+ (μ^-) and the direction opposite to that

[*]Full author list given at the end of the article.

of the B^0 ($\bar{B}^0$) in the rest frame of the dimuon system is denoted θ_l. The angle between the direction of the K^+ (K^-) and the B^0 ($\bar{B}^0$) in the rest frame of the K^{*0} ($\bar{K}^{*0}$) system is denoted θ_K. The angle between the plane defined by the dimuon pair and the plane defined by the kaon and pion in the B^0 ($\bar{B}^0$) rest frame is denoted ϕ. A full description of the angular basis is provided in Ref. [46].

Following the definitions given in Refs. [1,47], the CP-averaged angular distribution of the $B^0 \to K^{*0}\mu^+\mu^-$ decay with the $K^+\pi^-$ system in a P-wave configuration can be written as

$$\begin{aligned}\left.\frac{1}{d(\Gamma+\bar{\Gamma})/dq^2}\frac{d^4(\Gamma+\bar{\Gamma})}{dq^2 d\vec{\Omega}}\right|_P = \frac{9}{32\pi}\Bigg[&\frac{3}{4}(1-F_{\rm L})\sin^2\theta_K + F_{\rm L}\cos^2\theta_K + \frac{1}{4}(1-F_{\rm L})\sin^2\theta_K\cos 2\theta_l \\ &- F_{\rm L}\cos^2\theta_K\cos 2\theta_l + S_3\sin^2\theta_K\sin^2\theta_l\cos 2\phi + S_4\sin 2\theta_K\sin 2\theta_l\cos\phi + S_5\sin 2\theta_K\sin\theta_l\cos\phi \\ &+ \frac{4}{3}A_{\rm FB}\sin^2\theta_K\cos\theta_l + S_7\sin 2\theta_K\sin\theta_l\sin\phi + S_8\sin 2\theta_K\sin 2\theta_l\sin\phi + S_9\sin^2\theta_K\sin^2\theta_l\sin 2\phi\Bigg],\end{aligned} \tag{1}$$

where F_L is the fraction of the longitudinal polarization of the K^{*0} meson, $A_{\rm FB}$ is the forward-backward asymmetry of the dimuon system, and S_i are other CP-averaged observables [1]. The $K^+\pi^-$ system can also be in an S-wave configuration, which modifies the angular distribution to

$$\begin{aligned}\left.\frac{1}{d(\Gamma+\bar{\Gamma})/dq^2}\frac{d^4(\Gamma+\bar{\Gamma})}{dq^2 d\vec{\Omega}}\right|_{S+P} = (1-F_{\rm S})\frac{1}{d(\Gamma+\bar{\Gamma})/dq^2}\left.\frac{d^4(\Gamma+\bar{\Gamma})}{dq^2 d\vec{\Omega}}\right|_P + \frac{3}{16\pi}F_{\rm S}\sin^2\theta_l + \frac{9}{32\pi}(S_{11}+S_{13}\cos 2\theta_l)\cos\theta_K \\ + \frac{9}{32\pi}(S_{14}\sin 2\theta_l + S_{15}\sin\theta_l)\sin\theta_K\cos\phi + \frac{9}{32\pi}(S_{16}\sin\theta_l + S_{17}\sin 2\theta_l)\sin\theta_K\sin\phi,\end{aligned} \tag{2}$$

where F_S denotes the S-wave fraction and the coefficients S_{11}, S_{13}–S_{17} arise from interference between the S- and P-wave amplitudes. Throughout this Letter, F_S and the interference terms between the S and P wave are treated as nuisance parameters.

Additional sets of observables, for which the leading $B^0 \to K^{*0}$ form-factor uncertainties cancel, can be built from F_L, $A_{\rm FB}$, and S_3–S_9. Examples of such *optimized* observables include the $P_i^{(\prime)}$ series of observables [48]. The notation used in this Letter again follows Ref. [1], for example, $P_5' = S_5/\sqrt{F_L(1-F_L)}$.

The LHCb detector is a single-arm forward spectrometer covering the pseudorapidity range $2 < \eta < 5$, described in detail in Refs. [49,50]. The detector includes a vertex detector surrounding the proton-proton interaction region, tracking stations on either side of a dipole magnet, ring-imaging Cherenkov (RICH) detectors, electromagnetic and hadronic calorimeters, and muon chambers.

Simulated signal events are used in this analysis to determine the impact of the detector geometry, trigger, reconstruction, and candidate selection on the angular distribution of the signal. The simulation is produced using the software described in Refs. [51–56]. Corrections derived from the data are applied to the simulation to account for mismodeling of the charge multiplicity of the event, B^0 momentum spectrum, and B^0 vertex quality. Similarly, the simulated particle identification (PID) performance is corrected to match that determined from control samples selected from the data [57,58].

The online event selection is performed by a trigger, which comprises a hardware stage, based on information from the calorimeter and muon systems, followed by a software stage that applies a full event reconstruction [59]. Offline, signal candidates are formed from a pair of oppositely charged tracks that are identified as muons, combined with a K^{*0} candidate.

The distribution of the reconstructed $K^+\ \pi^-\ \mu^+\mu^-$ invariant mass, $m(K^+\pi^-\mu^+\mu^-)$, is used to discriminate signal from background. This distribution is fitted simultaneously with the three decay angles. The distribution of the reconstructed $K^+\pi^-$ mass, $m(K^+\pi^-)$, depends on the $K^+\pi^-$ angular-momentum configuration and is used to constrain the S-wave fraction. The analysis procedure is cross-checked by performing a fit of the $b \to c\bar{c}s$ tree-level decay $B^0 \to J/\psi K^{*0}$, with $J/\psi \to \mu^+\mu^-$, which results in the same final-state particles. Hereafter, the $B^0 \to J/\psi(\to \mu^+\mu^-)K^{*0}$ decay and the equivalent decay via the $\psi(2S)$ resonance are denoted by $B^0 \to J/\psi K^{*0}$ and $B^0 \to \psi(2S)K^{*0}$, respectively.

Two types of backgrounds are considered: combinatorial background, where the selected particles do not originate from a single b-hadron decay; and peaking backgrounds, where a single decay is selected but with some of the final-state particles misidentified. The combinatorial background is distributed smoothly in $m(K^+\pi^-\mu^+\mu^-)$, whereas the peaking backgrounds can accumulate in specific regions of the reconstructed mass. In addition, the decays $B^0 \to J/\psi K^{*0}$, $B^0 \to \psi(2S)K^{*0}$, and $B^0 \to \phi(1020)(\to \mu^+\mu^-)K^{*0}$ are removed by rejecting events with q^2 in the ranges $8.0 < q^2 < 11.0\ \mathrm{GeV}^2/c^4$, $12.5 < q^2 < 15.0\ \mathrm{GeV}^2/c^4$, or $0.98 < q^2 < 1.10\ \mathrm{GeV}^2/c^4$.

The criteria used to select candidates from the Run 1 data are the same as those described in Ref. [1]. The selection of the 2016 data follows closely that of the Run 1 data. Candidates are required to have $5170 < m(K^+\pi^-\mu^+\mu^-) < 5700$ and $795.9 < m(K^+\pi^-) < 995.9\ \mathrm{MeV}/c^2$. The four tracks of the final-state particles are required to have significant impact parameter (IP) with respect to all primary vertices (PVs) in the event. The tracks are fitted to a common vertex, which is required to be of good quality. The IP of the B^0 candidate is required to be small with respect to one of the PVs. The vertex of the B^0 candidate is required to be significantly displaced from the same PV. The angle between the reconstructed B^0 momentum and the vector connecting this PV to the reconstructed B^0 decay vertex, θ_{DIRA}, is also required to be small. To avoid the same track being used to construct more than one of the final state particles, the opening angle between every pair of tracks is required to be larger than 1 mrad.

Combinatorial background is reduced further using a boosted decision tree (BDT) algorithm [60,61]. The BDT is trained entirely on data with $B^0 \to J/\psi K^{*0}$ candidates used as a proxy for the signal and candidates from the upper-mass sideband $5350 < m(K^+\pi^-\mu^+\mu^-) < 7000\ \mathrm{MeV}/c^2$ used as a proxy for the background. The training uses a cross-validation technique [62] and is performed separately for the Run 1 and 2016 datasets. The input variables used are the reconstructed B^0 decay time and vertex-fit quality, the momentum and transverse momentum of the B^0 candidate θ_{DIRA}, PID information from the RICH detectors and the muon system, and variables describing the isolation of the final-state tracks [63]. Variables are only used in the BDT if they do not have a strong correlation with the decay angles or q^2. A requirement is placed on the BDT output to maximize the signal significance. This requirement rejects more than 97% of the remaining combinatorial background, while retaining more than 85% of the signal. The signal efficiency of the BDT is uniform in the $m(K^+\pi^-\mu^+\mu^-)$ and $m(K^+\pi^-)$ distributions.

Peaking backgrounds from $B_s^0 \to \phi(1020)(\to K^+K^-)\mu^+\mu^-$, $\Lambda_b^0 \to pK^-\mu^+\mu^-$, $B^0 \to J/\psi K^{*0}$, $B^0 \to \psi(2S)K^{*0}$, and $\bar{B}^0 \to \bar{K}^{*0}\mu^+\mu^-$ decays are considered, where the latter constitutes a background if the kaon from the $\bar{K}^{*0}$ decay is misidentified as the pion and vice versa. In each case, at least one particle needs to be misidentified for the decay to be reconstructed as a signal candidate. Vetoes to reduce these peaking backgrounds are formed by placing requirements on the invariant mass of the candidates, recomputed with the relevant change in the particle mass hypotheses, and by using PID information. In addition, in order to avoid having a strongly peaking contribution to the $\cos\theta_K$ angular distribution in the upper mass sideband, $B^+ \to K^+\mu^+\mu^-$ candidates with $K^+\mu^+\mu^-$ invariant mass within $60\ \mathrm{MeV}/c^2$ of the B^+ mass are removed. The background from b-hadron decays with two hadrons misidentified as muons is negligible. The signal efficiency and residual peaking backgrounds are estimated using simulated events. The vetoes remove a negligible amount of signal. The largest residual backgrounds are from $\bar{B}^0 \to \bar{K}^{*0}\mu^+\mu^-$, $\Lambda_b^0 \to pK^-\mu^+\mu^-$, and $B_s^0 \to \phi(1020)(\to K^+K^-)\mu^+\mu^-$ decays, at the level of 1% or less of the expected signal yield. This is sufficiently small such that these backgrounds are neglected in the angular analysis and are considered only as sources of systematic uncertainty.

For every q^2 bin, a fit is performed in both the standard and the optimized basis. For each basis, four datasets are fit simultaneously: the $m(K^+\pi^-\mu^+\mu^-)$ and angular distributions of candidates in the Run 1 data; the equivalent distributions for the 2016 data; and the $m(K^+\pi^-)$ distributions of candidates in the Run 1 and the 2016 datasets. The signal fraction is shared between the two datasets from each data-taking period. The CP-averaged angular observables and the S-wave fraction are shared between all datasets.

The fitted probability density functions (PDFs) are of an identical form to those of Ref. [1], as are the q^2 bins used. In addition to the narrow q^2 bins, results are obtained for the wider bins $1.1 < q^2 < 6.0$ and $15.0 < q^2 < 19.0\ \mathrm{GeV}^2/c^4$.

The angular distribution of the signal is described using Eq. (1). The $P_i^{(\prime)}$ observables are determined by reparametrizing Eq. (1) using a basis comprising F_L, $P_{1,2,3}$, and $P'_{4,5,6,8}$. The angular distribution is multiplied by an acceptance model used to account for the effect of the reconstruction and candidate selection. The acceptance function is parametrized in four dimensions, according to

$$\varepsilon(\cos\theta_l, \cos\theta_K, \phi, q^2) = \sum_{ijmn} c_{ijmn} L_i(\cos\theta_l) L_j(\cos\theta_K) L_m(\phi) L_n(q^2), \quad (3)$$

where the terms $L_h(x)$ denote Legendre polynomials of order h and the values of the angles and q^2 are rescaled to the range $-1 < x < +1$ when evaluating the polynomials. For the $\cos\theta_l$, $\cos\theta_K$, and ϕ angles, the sum in Eq. (3) encompasses $L_h(x)$ up to fourth, fifth, and sixth order, respectively. The q^2 parametrization comprises $L_h(x)$ up to

fifth order. Simulation indicates that the acceptance function can be assumed to be flat across $m(K^+\pi^-)$. The coefficients c_{ijmn} are determined using a principal moment analysis of simulated $B^0 \to K^{*0}\mu^+\mu^-$ decays. As all of the relevant kinematic variables needed to describe the decay are used in this parametrization, the acceptance function does not depend on the decay model used in the simulation.

In the narrow q^2 bins, the acceptance is taken to be constant across each bin and is included in the fit by multiplying Eq. (2) by the acceptance function evaluated with the value of q^2 fixed at the bin center. In the wider q^2 bins, the shape of the acceptance can vary significantly across the bin. In the likelihood, candidates are therefore weighted by the inverse of the acceptance function and parameter uncertainties are obtained using a bootstrapping technique [64].

The background angular distribution is modeled with second-order polynomials in $\cos\theta_l$, $\cos\theta_K$, and ϕ, with the angular coefficients allowed to vary in the fit. This angular distribution is assumed to factorize in the three decay angles, which is confirmed to be the case for candidates in the upper mass sideband of the data.

The $m(K^+\pi^-\mu^+\mu^-)$ distribution of the signal candidates is modeled using the sum of two Gaussian functions with a common mean, each with a power-law tail on the low mass side. The parameters describing the signal mass shape are determined from a fit to the $B^0 \to J/\psi K^{*0}$ decay in the data and are subsequently fixed when fitting the $B^0 \to K^{*0}\mu^+\mu^-$ candidates. For each of the q^2 bins, a scale factor that is determined from simulation is included to account for the difference in resolution between the $B^0 \to J/\psi K^{*0}$ and $B^0 \to K^{*0}\mu^+\mu^-$ decay modes. A component is included in the $B^0 \to J/\psi K^{*0}$ fit to account for $\bar{B}^0_s \to J/\psi K^{*0}$ decays, which are at the level of $\sim$1% of the $B^0 \to J/\psi K^{*0}$ signal yield. The background from the equivalent Cabibbo-suppressed penguin decay, $\bar{B}^0_s \to K^{*0}\mu^+\mu^-$ [65], is negligible and is ignored in the fit of the signal decay. The combinatorial background is described well by an exponential distribution in $m(K^+\pi^-\mu^+\mu^-)$.

The K^{*0} signal component in the $m(K^+\pi^-)$ distribution is modeled using a relativistic Breit-Wigner function for the P-wave component and the LASS parametrization [66] for the S-wave component. The combinatorial background is described by a linear function in $m(K^+\pi^-)$.

The decay $B^0 \to J/\psi K^{*0}$ is used to cross-check the analysis procedure in the region $8.0 < q^2 < 11.0\ \mathrm{GeV}^2/c^4$. This decay is selected in the data with negligible background contamination. The angular structure has been determined by measurements made by the *BABAR*, Belle, and LHCb Collaborations [67–69]. The $B^0 \to J/\psi K^{*0}$ angular observables obtained from the Run 1 and 2016 LHCb data, using the acceptance correction derived as described above, are in good agreement with these previous measurements.

Figure 1 shows the projection of the fitted PDF on the $K^+\,\pi^-\,\mu^+\mu^-$ mass distribution. The $B^0 \to K^{*0}\mu^+\mu^-$ yield, integrated over the q^2 ranges $0.10 < q^2 < 0.98$, $1.1 < q^2 < 8.0$, $11.0 < q^2 < 12.5$, and $15.0 < q^2 < 19.0\ \mathrm{GeV}^2/c^4$, is determined to be 2398 ± 57 for the Run 1 data, and 2187 ± 53 for the 2016 data.

Pseudoexperiments, generated using the results of the best fit to data, are used to assess the bias and coverage of the fit. The majority of observables have a bias of less than 10% of their statistical uncertainty, with the largest bias being 17%, and all observables have an uncertainty estimate within 10% of the true uncertainty. The biases are driven by boundary effects in the observables. The largest effect comes from requiring that $F_S \geq 0$, which can bias F_S to larger values. This can then result in a bias in the P-wave observables [see Eq. (2)]. The statistical uncertainty is corrected to account for any under- or over-coverage and a systematic uncertainty equal to the size of the observed bias is assigned.

The size of other sources of systematic uncertainty is estimated using pseudoexperiments, in which one or more parameters are varied and the angular observables are determined with and without this variation. The systematic uncertainty is then taken as the difference between the two

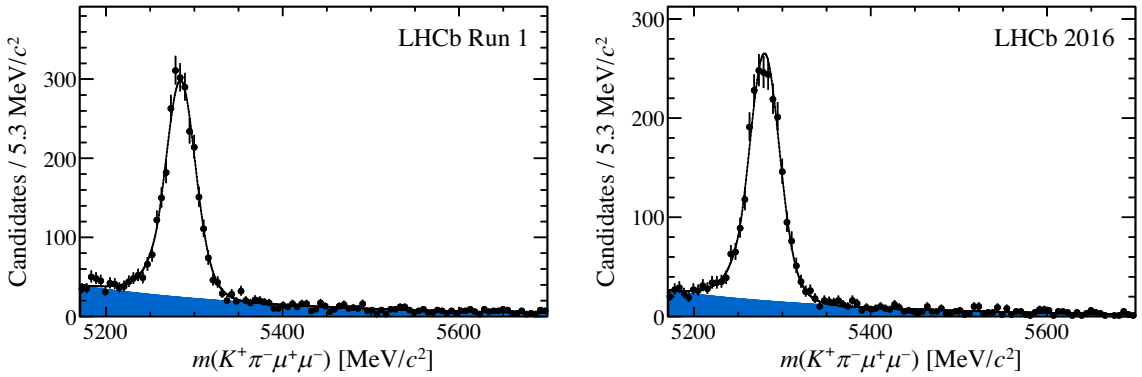

FIG. 1. The $K^+\pi^-\mu^+\mu^-$ mass distribution of candidates with $0.1 < q^2 < 19.0\ \mathrm{GeV}^2/c^4$, excluding the $\phi(1020)$ and charmonium regions, for the (left) Run 1 data and (right) 2016 data. The background is indicated by the shaded region.

models. The pseudoexperiments are generated with signal yields many times larger than the data, in order to render statistical fluctuations negligible.

The size of the total systematic uncertainty varies depending on the angular observable and the q^2 bin. The majority of observables in both the S_i and $P_i^{(\prime)}$ basis have a total systematic uncertainty between 5% and 25% of the statistical uncertainty. For F_L, the systematic uncertainty tends to be larger, typically between 20% and 50%. The systematic uncertainties are given in Table 3 of Ref. [70].

The dominant systematic uncertainties arise from the peaking backgrounds that are neglected in the analysis, the bias correction, and, for the narrow q^2 bins, from the uncertainty associated with evaluating the acceptance at a fixed point in q^2. For the peaking backgrounds, the systematic uncertainty is evaluated by injecting additional candidates, drawn from the angular distributions of the background modes, into the pseudoexperiment data. The systematic uncertainty for the bias correction is determined directly from the pseudoexperiments used to validate the fit. The systematic uncertainty from the variation of the acceptance with q^2 is determined by moving the point in q^2 at which the acceptance is evaluated to halfway between the bin center and the upper or the lower edge. The largest deviation is taken as the systematic uncertainty. Examples of further sources of systematic uncertainty investigated include the $m(K^+\pi^-)$ line shape for the S-wave contribution, the assumption that the acceptance function is flat across the $m(K^+\pi^-)$ mass, the effect of the $B^+ \to K^+\mu^+\mu^-$ veto on the angular distribution of the background and the order of polynomial used for the background parametrization. These sources make a negligible contribution to the total uncertainty. With respect to the analysis of Ref. [1], the systematic uncertainty from residual differences between data and simulation is significantly reduced, owing to an improved decay model for $B^0 \to J/\psi K^{*0}$ decays [68].

The CP-averaged observables F_L, $A_{\rm FB}$, S_5, and P_5' that are obtained from the S_i and $P_i^{(\prime)}$ fits are shown together with their respective SM predictions in Fig. 2. The results for all observables are given in Figs. 1 and 2 and Tables 1 and 2 of Ref. [70]. In addition, the statistical correlation between the observables is provided in Tables 4–23. The SM predictions are based on the prescription of Ref. [44], which combines light-cone sum rule calculations [43], valid in the low-q^2 region, with lattice determinations at high q^2 [71,72] to yield more precise determinations of the form factors over the full q^2 range. For the $P_i^{(\prime)}$ observables, predictions from Ref. [73] are shown using form factors

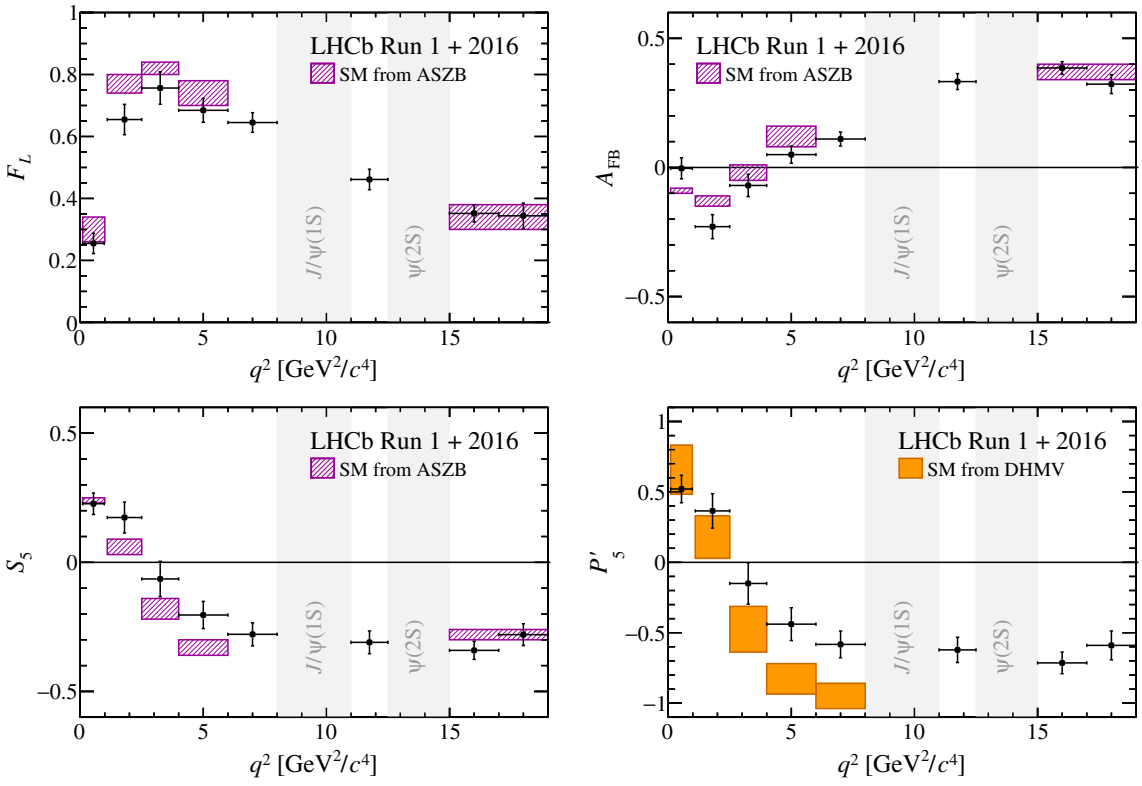

FIG. 2. Results for the CP-averaged angular observables F_L, $A_{\rm FB}$, S_5, and P_5' in bins of q^2. The data are compared to SM predictions based on the prescription of Refs. [43,44], with the exception of the P_5' distribution, which is compared to SM predictions based on Refs. [73,74].

from Ref. [74]. These predictions are restricted to the region $q^2 < 8.0\ \mathrm{GeV}^2/c^4$. The results from Run 1 and the 2016 data are in excellent agreement. A stand-alone fit to the Run 1 data reproduces exactly the central values of the observables obtained in Ref. [1].

Considering the observables individually, the results are largely in agreement with the SM predictions. The local discrepancy in the P_5' observable in the $4.0 < q^2 < 6.0$ and $6.0 < q^2 < 8.0\ \mathrm{GeV}^2/c^4$ bins reduces from the 2.8 and 3.0σ observed in Ref. [1] to 2.5 and 2.9σ. However, as discussed below, the overall tension with the SM is observed to increase mildly.

Using the FLAVIO software package [42], a fit of the angular observables is performed varying the parameter $\mathcal{R}e(C_9)$. The default FLAVIO SM nuisance parameters are used, including form-factor parameters and subleading corrections to account for long-distance QCD interference effects with the charmonium decay modes [43,44]. The same q^2 bins as in Ref. [1] are included. The 3.0σ discrepancy with respect to the SM value of $\mathcal{R}e(C_9)$ obtained with the Ref. [1] dataset changes to 3.3σ with the dataset used here. The best fit to the angular distribution is obtained with a shift in the SM value of $\mathcal{R}e(C_9)$ by $-0.99^{+0.25}_{-0.21}$. The tension observed in any such fit will depend on the effective coupling(s) varied, the handling of the SM nuisance parameters, and the q^2 bins that are included in the fit. For example, the $6.0 < q^2 < 8.0\ \mathrm{GeV}^2/c^4$ bin is known to be associated with larger theoretical uncertainties [47]. Neglecting this bin, a FLAVIO fit gives a tension of 2.4σ using the observables from Ref. [1] and 2.7σ tension with the measurements reported here.

In summary, using $4.7\ \mathrm{fb}^{-1}$ of pp collision data collected with the LHCb experiment during the years 2011, 2012, and 2016, a complete set of CP-averaged angular observables has been measured for the $B^0 \to K^{*0}\mu^+\mu^-$ decay. These are the most precise measurements of these quantities to date.

We express our gratitude to our colleagues in the CERN accelerator departments for the excellent performance of the LHC. We thank the technical and administrative staff at the LHCb institutes. We acknowledge support from CERN and from the national agencies: CAPES, CNPq, FAPERJ and FINEP (Brazil); MOST and NSFC (China); CNRS/IN2P3 (France); BMBF, DFG and MPG (Germany); INFN (Italy); NWO (Netherlands); MNiSW and NCN (Poland); MEN/IFA (Romania); MSHE (Russia); MinECo (Spain); SNSF and SER (Switzerland); NASU (Ukraine); STFC (United Kingdom); DOE NP and NSF (USA). We acknowledge the computing resources that are provided by CERN, IN2P3 (France), KIT and DESY (Germany), INFN (Italy), SURF (Netherlands), PIC (Spain), GridPP (United Kingdom), RRCKI and Yandex LLC (Russia), CSCS (Switzerland), IFIN-HH (Romania), CBPF (Brazil), PL-GRID (Poland) and OSC (USA). We are indebted to the communities behind the multiple open-source software packages on which we depend. Individual groups or members have received support from AvH Foundation (Germany); EPLANET, Marie Skłodowska-Curie Actions and ERC (European Union); ANR, Labex P2IO and OCEVU, and Région Auvergne-Rhône-Alpes (France); Key Research Program of Frontier Sciences of CAS, CAS PIFI, and the Thousand Talents Program (China); RFBR, RSF and Yandex LLC (Russia); GVA, XuntaGal and GENCAT (Spain); the Royal Society and the Leverhulme Trust (United Kingdom).

[1] R. Aaij *et al.* (LHCb Collaboration), Angular analysis of the $B^0 \to K^{*0}\mu^+\mu^-$ decay using 3 fb^{-1} of integrated luminosity, J. High Energy Phys. 02 (2016) 104.

[2] A. M. Sirunyan *et al.* (CMS Collaboration), Measurement of angular parameters from the decay $B^0 \to K^{*0}\mu^+\mu^-$ in proton-proton collisions at $\sqrt{s} = 8$ TeV, Phys. Lett. B **781**, 517 (2018).

[3] M. Aaboud *et al.* (ATLAS Collaboration), Angular analysis of $B_d^0 \to K^*\mu^+\mu^-$ decays in pp collisions at $\sqrt{s} = 8$ TeV with the ATLAS detector, J. High Energy Phys. 10 (2018) 047.

[4] S. Wehle *et al.* (Belle Collaboration), Lepton-Flavor-Dependent Angular Analysis of $B \to K^*\ell^+\ell^-$, Phys. Rev. Lett. **118**, 111801 (2017).

[5] B. Aubert *et al.* (*BABAR* Collaboration), Measurements of branching fractions, rate asymmetries, and angular distributions in the rare decays $B \to K\ell^+\ell^-$ and $B \to K^*\ell^+\ell^-$, Phys. Rev. D **73**, 092001 (2006).

[6] T. Aaltonen *et al.* (CDF Collaboration), Measurements of the Angular Distributions in the Decays $B \to K^{(*)}\mu^+\mu^-$ at CDF, Phys. Rev. Lett. **108**, 081807 (2012).

[7] R. Aaij *et al.* (LHCb Collaboration), Angular moments of the decay $\Lambda_b^0 \to \Lambda\mu^+\mu^-$ at low hadronic recoil, J. High Energy Phys. 09 (2018) 146.

[8] R. Aaij *et al.* (LHCb Collaboration), Angular analysis and differential branching fraction of the decay $B_s^0 \to \phi\mu^+\mu^-$, J. High Energy Phys. 09 (2015) 179.

[9] R. Aaij *et al.* (LHCb Collaboration), Measurements of the S-wave fraction in $B^0 \to K^+\pi^-\mu^+\mu^-$ decays and the $B^0 \to K^*(892)^0\mu^+\mu^-$ differential branching fraction, J. High Energy Phys. 11 (2016) 047; 04 (2017) 142(E).

[10] R. Aaij *et al.* (LHCb Collaboration), Differential branching fraction and angular analysis of $\Lambda_b^0 \to \Lambda\mu^+\mu^-$ decays, J. High Energy Phys. 06 (2015) 115; 09 (2018) 145(E).

[11] R. Aaij *et al.* (LHCb Collaboration), Differential branching fractions and isospin asymmetries of $B \to K^{(*)}\mu^+\mu^-$ decays, J. High Energy Phys. 06 (2014) 133.

[12] R. Aaij *et al.* (LHCb Collaboration), Search for Lepton-Universality Violation in $B^+ \to K^+\ell^+\ell^-$ Decays, Phys. Rev. Lett. **122**, 191801 (2019).

[13] A. Abdesselam *et al.* (Belle Collaboration), Test of lepton flavor universality in $B \to K\ell^+\ell^-$ decays, arXiv:1908.01848.

[14] J. P. Lees *et al.* (*BABAR* Collaboration), Measurement of branching fractions and rate asymmetries in the rare decays $B \to K^{(*)}\ell^+\ell^-$, Phys. Rev. D **86**, 032012 (2012).

[15] R. Aaij *et al.* (LHCb Collaboration), Test of lepton universality with $B^0 \to K^{*0}\ell^+\ell^-$ decays, J. High Energy Phys. 08 (2017) 055.

[16] A. Abdesselam *et al.* (Belle Collaboration), Test of lepton flavor universality in $B \to K^*\ell^+\ell^-$ decays at Belle, arXiv:1904.02440.

[17] M. Algueró, B. Capdevila, A. Crivellin, S. Descotes-Genon, P. Masjuan, J. Matias, and J. Virto, Emerging patterns of new physics with and without Lepton flavour universal contributions, Eur. Phys. J. C **79**, 714 (2019).

[18] J. Aebischer *et al.*, B-decay discrepancies after Moriond 2019, Eur. Phys. J. C **80**, 252 (2020).

[19] A. Arbey, T. Hurth, F. Mahmoudi, D. M. Santos, and S. Neshatpour, Update on the $b \to s$ anomalies, Phys. Rev. D **100**, 015045 (2019).

[20] M. Ciuchini, A. M. Coutinho, M. Fedele, E. Franco, A. Paul, L. Silvestrini, and M. Valli, New physics in $b \to s\ell^+\ell^-$ confronts new data on lepton universality, Eur. Phys. J. C **79**, 719 (2019).

[21] K. Kowalska, D. Kumar, and E. M. Sessolo, Implications for new physics in $b \to s\mu\mu$ transitions after recent measurements by Belle and LHCb, Eur. Phys. J. C **79**, 840 (2019).

[22] A. K. Alok, A. Dighe, S. Gangal, and D. Kumar, Continuing search for new physics in $b \to s\mu\mu$ decays: Two operators at a time, J. High Energy Phys. 06 (2019) 089.

[23] W. Altmannshofer, S. Gori, M. Pospelov, and I. Yavin, Quark flavor transitions in $L_\mu - L_\tau$ models, Phys. Rev. D **89**, 095033 (2014).

[24] A. Crivellin, G. D'Ambrosio, and J. Heeck, Explaining $h \to \mu^\pm\tau^\mp$, $B \to K^*\mu^+\mu^-$ and $B \to K\mu^+\mu^-/B \to Ke^+e^-$ in a Two-Higgs-Doublet Model with Gauged $L_\mu - L_\tau$, Phys. Rev. Lett. **114**, 151801 (2015).

[25] A. Celis, J. Fuentes-Martín, M. Jung, and H. Serôdio, Family nonuniversal Z' models with protected flavor-changing interactions, Phys. Rev. D **92**, 015007 (2015).

[26] A. Falkowski, M. Nardecchia, and R. Ziegler, Lepton flavor non-universality in B-meson decays from a $U(2)$ flavor model, J. High Energy Phys. 11 (2015) 173.

[27] G. Hiller and M. Schmaltz, R_K and future $b \to s\ell\ell$ physics beyond the standard model opportunities, Phys. Rev. D **90**, 054014 (2014).

[28] B. Gripaios, M. Nardecchia, and S. A. Renner, Composite leptoquarks and anomalies in B-meson decays, J. High Energy Phys. 05 (2015) 006.

[29] I. de Medeiros Varzielas and G. Hiller, Clues for flavor from rare lepton and quark decays, J. High Energy Phys. 06 (2015) 072.

[30] R. Barbieri, C. W. Murphy, and F. Senia, B-decay anomalies in a composite leptoquark model, Eur. Phys. J. C **77**, 8 (2017).

[31] J.-H. Sheng, R.-M. Wang, and Y.-D. Yang, Scalar leptoquark effects in the lepton flavor violating exclusive $b \to s\ell_i^-\ell_j^+$ Decays, Int. J. Theor. Phys. **58**, 480 (2019).

[32] G. Hiller, D. Loose, and I. Nişandžić, Flavorful leptoquarks at hadron colliders, Phys. Rev. D **97**, 075004 (2018).

[33] A. Crivellin, D. Müller, and T. Ota, Simultaneous explanation of $R(D^{(*)})$ and $b \to s\mu^+\mu^-$: The last scalar leptoquarks standing, J. High Energy Phys. 09 (2017) 040.

[34] F. Sala and D. M. Straub, A new light particle in B decays?, Phys. Lett. B **774**, 205 (2017).

[35] P. Ko, Y. Omura, Y. Shigekami, and C. Yu, LHCb anomaly and B physics in flavored Z' models with flavored Higgs doublets, Phys. Rev. D **95**, 115040 (2017).

[36] S. Jäger and J. Martin Camalich, Reassessing the discovery potential of the $B \to K^*\ell^+\ell^-$ decays in the large-recoil region: SM challenges and BSM opportunities, Phys. Rev. D **93**, 014028 (2016).

[37] J. Lyon and R. Zwicky, Resonances gone topsy turvy—the charm of QCD or new physics in $b \to s\ell^+\ell^-$?, arXiv:1406.0566.

[38] M. Ciuchini, M. Fedele, E. Franco, S. Mishima, A. Paul, L. Silvestrini, and M. Valli, $B \to K^*\ell^+\ell^-$ decays at large recoil in the Standard Model: A theoretical reappraisal, J. High Energy Phys. 06 (2016) 116.

[39] C. Bobeth, M. Chrzaszcz, D. van Dyk, and J. Virto, Long-distance effects in $B \to K^*\ell\ell$ from analyticity, Eur. Phys. J. C **78**, 451 (2018).

[40] F. Beaujean, C. Bobeth, and D. van Dyk, Comprehensive Bayesian analysis of rare (semi)leptonic and radiative B decays, Eur. Phys. J. C **74**, 2897 (2014).

[41] C. Bobeth, G. Hiller, and D. van Dyk, The benefits of $\bar{B} \to \bar{K}^* l^+ l^-$ decays at low recoil, J. High Energy Phys. 07 (2010) 098.

[42] D. M. Straub, flavio: A python package for flavour and precision phenomenology in the Standard Model and beyond, arXiv:1810.08132.

[43] A. Bharucha, D. M. Straub, and R. Zwicky, $B \to V\ell^+\ell^-$ in the Standard Model from light-cone sum rules, J. High Energy Phys. 08 (2016) 098.

[44] W. Altmannshofer and D. M. Straub, New physics in $b \to s$ transitions after LHC Run 1, Eur. Phys. J. C **75**, 382 (2015).

[45] R. Aaij *et al.* (LHCb collaboration), Measurement of the $B^\pm$ production cross-section in pp collisions at $\sqrt{s} = 7$ and 13 TeV, J. High Energy Phys. 12 (2017) 026.

[46] R. Aaij *et al.* (LHCb collaboration), Differential branching fraction and angular analysis of the decay $B^0 \to K^{*0}\mu^+\mu^-$, J. High Energy Phys. 08 (2013) 131.

[47] W. Altmannshofer, P. Ball, A. Bharucha, A. J. Buras, D. M. Straub, and M. Wick, Symmetries and asymmetries of $B \to K^*\mu^+\mu^-$ decays in the Standard Model and beyond, J. High Energy Phys. 01 (2009) 019.

[48] S. Descotes-Genon, J. Matias, M. Ramon, and J. Virto, Implications from clean observables for the binned analysis of $B \to K^*\mu^+\mu^-$ at large recoil, J. High Energy Phys. 01 (2013) 048.

[49] A. A. Alves, Jr. *et al.* (LHCb Collaboration), The LHCb detector at the LHC, J. Instrum. **3**, S08005 (2008).

[50] R. Aaij *et al.* (LHCb Collaboration), LHCb detector performance, Int. J. Mod. Phys. A **30**, 1530022 (2015).

[51] T. Sjöstrand, S. Mrenna, and P. Skands, PYTHIA 6.4 physics and manual, J. High Energy Phys. 05 (2006) 026; T. Sjöstrand, S. Mrenna, and P. Skands, A brief introduction to PYTHIA 8.1, Comput. Phys. Commun. **178**, 852 (2008).

[52] I. Belyaev *et al.*, Handling of the generation of primary events in Gauss, the LHCb simulation framework, J. Phys. Conf. Ser. **331**, 032047 (2011).

[53] D. J. Lange, The EvtGen particle decay simulation package, Nucl. Instrum. Methods Phys. Res., Sect. A **462**, 152 (2001).

[54] P. Golonka and Z. Was, PHOTOS Monte Carlo: A precision tool for QED corrections in Z and W decays, Eur. Phys. J. C **45**, 97 (2006).

[55] J. Allison *et al.* (Geant4 Collaboration), Geant4 developments and applications, IEEE Trans. Nucl. Sci. **53** (2006) 270; S. Agostinelli *et al.* (Geant4 Collaboration), Geant4: A simulation toolkit, Nucl. Instrum. Methods Phys. Res., Sect. A **506**, 250 (2003).

[56] M. Clemencic, G. Corti, S. Easo, C. R. Jones, S. Miglioranzi, M. Pappagallo, and P. Robbe, The LHCb simulation application, Gauss: Design, evolution and experience, J. Phys. Conf. Ser. **331**, 032023 (2011).

[57] L. Anderlini *et al.*, The PIDCalib package, CERN Report No. LHCb-PUB-2016-021, Geneva, 2016, https://cds.cern.ch/record/2202412.

[58] R. Aaij *et al.*, Selection and processing of calibration samples to measure the particle identification performance of the LHCb experiment in Run 2, EPJ Tech. Instrum. **6**, 1 (2019).

[59] R. Aaij *et al.*, The LHCb trigger and its performance in 2011, J. Instrum. **8**, P04022 (2013).

[60] L. Breiman, J. H. Friedman, R. A. Olshen, and C. J. Stone, *Classification and Regression Trees* (Wadsworth International Group, Belmont, California, USA, 1984).

[61] Y. Freund and R. E. Schapire, A decision-theoretic generalization of on-line learning and an application to boosting, J. Comput. Syst. Sci. **55**, 119 (1997).

[62] A. Blum, A. Kalai, and J. Langford, Beating the hold-out: Bounds for k-fold and progressive cross-validation, in *Proceedings of the Twelfth Annual Conference on Computational Learning Theory*, COLT '99 (ACM, New York, NY, 1999), pp. 203–208, https://doi.org/10.1145/307400.307439.

[63] R. Aaij *et al.* (LHCb Collaboration), Search for the rare decays $B_s^0 \to \mu^+\mu^-$ and $B^0 \to \mu^+\mu^-$, Phys. Lett. B **699**, 330 (2011).

[64] B. Efron, Bootstrap methods: Another look at the jackknife, Ann. Stat. **7**, 1 (1979).

[65] R. Aaij *et al.* (LHCb Collaboration), Evidence for the decay $B_s^0 \to \bar{K}^{*0}\mu^+\mu^-$, J. High Energy Phys. 07 (2018) 020.

[66] D. Aston *et al.*, A Study of $K^-\pi^+$ scattering in the reaction $K^-\pi^+ \to K^-\pi^+ n$ at 11 GeV/c, Nucl. Phys. **B296**, 493 (1988).

[67] B. Aubert *et al.* (*BABAR* Collaboration), Measurement of decay amplitudes of $B \to J/\psi K^*$, $\psi(2S)K^*$, and $\chi_{c1}K^*$ with an angular analysis, Phys. Rev. D **76**, 031102 (2007).

[68] K. Chilikin *et al.* (Belle Collaboration), Observation of a new charged charmonium like state in $\bar{B}^0 \to J/\psi K^-\pi^+$ decays, Phys. Rev. D **90**, 112009 (2014).

[69] R. Aaij *et al.* (LHCb Collaboration), Measurement of the polarization amplitudes in $B^0 \to J/\psi K^*(892)^0$ decays, Phys. Rev. D **88**, 052002 (2013).

[70] See Supplemental Material at http://link.aps.org/supplemental/10.1103/PhysRevLett.125.011802 for full set of results for the nominal analysis, a complete description of the systematics, the correlations between the angular observables, and the angular and mass distributions of the selected candidates.

[71] R. R. Horgan, Z. Liu, S. Meinel, and M. Wingate, Lattice QCD calculation of form factors describing the rare decays $B \to K^*\ell^+\ell^-$ and $B_s \to \phi\ell^+\ell^-$, Phys. Rev. D **89**, 094501 (2014).

[72] R. R. Horgan, Z. Liu, S. Meinel, and M. Wingate, Rare B decays using lattice QCD form factors, Proc. Sci. LATTICE2014 (**2015**) 372.

[73] S. Descotes-Genon, L. Hofer, J. Matias, and J. Virto, On the impact of power corrections in the prediction of $B \to K^*\mu^+\mu^-$ observables, J. High Energy Phys. 12 (2014) 125.

[74] A. Khodjamirian, T. Mannel, A. A. Pivovarov, and Y.-M. Wang, Charm-loop effect in $B \to K^{(*)}\ell^+\ell^-$ and $B \to K^*\gamma$, J. High Energy Phys. 09 (2010) 089.

R. Aaij,[31] C. Abellán Beteta,[49] T. Ackernley,[59] B. Adeva,[45] M. Adinolfi,[53] H. Afsharnia,[9] C. A. Aidala,[81] S. Aiola,[25] Z. Ajaltouni,[9] S. Akar,[66] P. Albicocco,[22] J. Albrecht,[14] F. Alessio,[47] M. Alexander,[58] A. Alfonso Albero,[44] G. Alkhazov,[37] P. Alvarez Cartelle,[60] A. A. Alves Jr.,[45] S. Amato,[2] Y. Amhis,[11] L. An,[21] L. Anderlini,[21] G. Andreassi,[48] M. Andreotti,[20] F. Archilli,[16] A. Artamonov,[43] M. Artuso,[67] K. Arzymatov,[41] E. Aslanides,[10] M. Atzeni,[49] B. Audurier,[11] S. Bachmann,[16] J. J. Back,[55] S. Baker,[60] V. Balagura,[11,a] W. Baldini,[20] A. Baranov,[41] R. J. Barlow,[61] S. Barsuk,[11] W. Barter,[60] M. Bartolini,[23,47,b] F. Baryshnikov,[78] J. M. Basels,[13] G. Bassi,[28] V. Batozskaya,[35] B. Batsukh,[67] A. Battig,[14] A. Bay,[48] M. Becker,[14] F. Bedeschi,[28] I. Bediaga,[1] A. Beiter,[67] V. Belavin,[41] S. Belin,[26] V. Bellee,[48] K. Belous,[43] I. Belyaev,[38] G. Bencivenni,[22] E. Ben-Haim,[12] S. Benson,[31] A. Berezhnoy,[39] R. Bernet,[49] D. Berninghoff,[16] H. C. Bernstein,[67] C. Bertella,[47] E. Bertholet,[12] A. Bertolin,[27] C. Betancourt,[49] F. Betti,[19,c] M. O. Bettler,[54] Ia. Bezshyiko,[49] S. Bhasin,[53] J. Bhom,[33] M. S. Bieker,[14] S. Bifani,[52] P. Billoir,[12] A. Bizzeti,[21,d] M. Bjørn,[62] M. P. Blago,[47] T. Blake,[55] F. Blanc,[48] S. Blusk,[67] D. Bobulska,[58] V. Bocci,[30] O. Boente Garcia,[45] T. Boettcher,[63] A. Boldyrev,[79] A. Bondar,[42,e] N. Bondar,[37,47] S. Borghi,[61] M. Borisyak,[41] M. Borsato,[16] J. T. Borsuk,[33] T. J. V. Bowcock,[59] C. Bozzi,[20] M. J. Bradley,[60] S. Braun,[65] A. Brea Rodriguez,[45] M. Brodski,[47] J. Brodzicka,[33] A. Brossa Gonzalo,[55] D. Brundu,[26] E. Buchanan,[53] A. Büchler-Germann,[49] A. Buonaura,[49] C. Burr,[47] A. Bursche,[26] A. Butkevich,[40] J. S. Butter,[31] J. Buytaert,[47] W. Byczynski,[47] S. Cadeddu,[26] H. Cai,[72] R. Calabrese,[20,f] L. Calero Diaz,[22] S. Cali,[22] R. Calladine,[52] M. Calvi,[24,g]

M. Calvo Gomez,[44,h] P. Camargo Magalhaes,[53] A. Camboni,[44,h] P. Campana,[22] D. H. Campora Perez,[31] A. F. Campoverde Quezada,[5] L. Capriotti,[19,c] A. Carbone,[19,c] G. Carboni,[29] R. Cardinale,[23,b] A. Cardini,[26] I. Carli,[6] P. Carniti,[24,g] K. Carvalho Akiba,[31] A. Casais Vidal,[45] G. Casse,[59] M. Cattaneo,[47] G. Cavallero,[47] S. Celani,[48] R. Cenci,[28,i] J. Cerasoli,[10] M. G. Chapman,[53] M. Charles,[12] Ph. Charpentier,[47] G. Chatzikonstantinidis,[52] M. Chefdeville,[8] V. Chekalina,[41] C. Chen,[3] S. Chen,[26] A. Chernov,[33] S.-G. Chitic,[47] V. Chobanova,[45] S. Cholak,[48] M. Chrzaszcz,[33] A. Chubykin,[37] V. Chulikov,[37] P. Ciambrone,[22] M. F. Cicala,[55] X. Cid Vidal,[45] G. Ciezarek,[47] F. Cindolo,[19] P. E. L. Clarke,[57] M. Clemencic,[47] H. V. Cliff,[54] J. Closier,[47] J. L. Cobbledick,[61] V. Coco,[47] J. A. B. Coelho,[11] J. Cogan,[10] E. Cogneras,[9] L. Cojocariu,[36] P. Collins,[47] T. Colombo,[47] A. Contu,[26] N. Cooke,[52] G. Coombs,[58] S. Coquereau,[44] G. Corti,[47] C. M. Costa Sobral,[55] B. Couturier,[47] D. C. Craik,[63] J. Crkovská,[66] A. Crocombe,[55] M. Cruz Torres,[1,j] R. Currie,[57] C. L. Da Silva,[66] E. Dall'Occo,[14] J. Dalseno,[45,53] C. D'Ambrosio,[47] A. Danilina,[38] P. d'Argent,[47] A. Davis,[61] O. De Aguiar Francisco,[47] K. De Bruyn,[47] S. De Capua,[61] M. De Cian,[48] J. M. De Miranda,[1] L. De Paula,[2] M. De Serio,[18,k] P. De Simone,[22] J. A. de Vries,[76] C. T. Dean,[66] W. Dean,[81] D. Decamp,[8] L. Del Buono,[12] B. Delaney,[54] H.-P. Dembinski,[14] A. Dendek,[34] V. Denysenko,[49] D. Derkach,[79] O. Deschamps,[9] F. Desse,[11] F. Dettori,[26,l] B. Dey,[7] A. Di Canto,[47] P. Di Nezza,[22] S. Didenko,[78] H. Dijkstra,[47] V. Dobishuk,[51] F. Dordei,[26] M. Dorigo,[28,m] A. C. dos Reis,[1] L. Douglas,[58] A. Dovbnya,[50] K. Dreimanis,[59] M. W. Dudek,[33] L. Dufour,[47] P. Durante,[47] J. M. Durham,[66] D. Dutta,[61] M. Dziewiecki,[16] A. Dziurda,[33] A. Dzyuba,[37] S. Easo,[56] U. Egede,[69] V. Egorychev,[38] S. Eidelman,[42,e] S. Eisenhardt,[57] S. Ek-In,[48] L. Eklund,[58] S. Ely,[67] A. Ene,[36] E. Epple,[66] S. Escher,[13] J. Eschle,[49] S. Esen,[31] T. Evans,[47] A. Falabella,[19] J. Fan,[3] Y. Fan,[5] N. Farley,[52] S. Farry,[59] D. Fazzini,[11] P. Fedin,[38] M. Féo,[47] P. Fernandez Declara,[47] A. Fernandez Prieto,[45] F. Ferrari,[19,c] L. Ferreira Lopes,[48] F. Ferreira Rodrigues,[2] S. Ferreres Sole,[31] M. Ferrillo,[49] M. Ferro-Luzzi,[47] S. Filippov,[40] R. A. Fini,[18] M. Fiorini,[20,f] M. Firlej,[34] K. M. Fischer,[62] C. Fitzpatrick,[47] T. Fiutowski,[34] F. Fleuret,[11,a] M. Fontana,[47] F. Fontanelli,[23,b] R. Forty,[47] V. Franco Lima,[59] M. Franco Sevilla,[65] M. Frank,[47] C. Frei,[47] D. A. Friday,[58] J. Fu,[25,n] Q. Fuehring,[14] W. Funk,[47] E. Gabriel,[57] T. Gaintseva,[41] A. Gallas Torreira,[45] D. Galli,[19,c] S. Gallorini,[27] S. Gambetta,[57] Y. Gan,[3] M. Gandelman,[2] P. Gandini,[25] Y. Gao,[4] L. M. Garcia Martin,[46] J. García Pardiñas,[49] B. Garcia Plana,[45] F. A. Garcia Rosales,[11] L. Garrido,[44] D. Gascon,[44] C. Gaspar,[47] D. Gerick,[16] E. Gersabeck,[61] M. Gersabeck,[61] T. Gershon,[55] D. Gerstel,[10] Ph. Ghez,[8] V. Gibson,[54] A. Gioventù,[45] P. Gironella Gironell,[44] L. Giubega,[36] C. Giugliano,[20] K. Gizdov,[57] V. V. Gligorov,[12] C. Göbel,[70] D. Golubkov,[38] A. Golutvin,[60,78] A. Gomes,[1,o] P. Gorbounov,[38] I. V. Gorelov,[39] C. Gotti,[24,g] E. Govorkova,[31] J. P. Grabowski,[16] R. Graciani Diaz,[44] T. Grammatico,[12] L. A. Granado Cardoso,[47] E. Graugés,[44] E. Graverini,[48] G. Graziani,[21] A. Grecu,[36] R. Greim,[31] P. Griffith,[20] L. Grillo,[61] L. Gruber,[47] B. R. Gruberg Cazon,[62] C. Gu,[3] E. Gushchin,[40] A. Guth,[13] Yu. Guz,[43,47] T. Gys,[47] P. A. Günther,[16] T. Hadavizadeh,[62] G. Haefeli,[48] C. Haen,[47] S. C. Haines,[54] P. M. Hamilton,[65] Q. Han,[7] X. Han,[16] T. H. Hancock,[62] S. Hansmann-Menzemer,[16] N. Harnew,[62] T. Harrison,[59] R. Hart,[31] C. Hasse,[14] M. Hatch,[47] J. He,[5] M. Hecker,[60] K. Heijhoff,[31] K. Heinicke,[14] A. M. Hennequin,[47] K. Hennessy,[59] L. Henry,[25,46] J. Heuel,[13] A. Hicheur,[68] D. Hill,[62] M. Hilton,[61] P. H. Hopchev,[48] J. Hu,[16] J. Hu,[71] W. Hu,[7] W. Huang,[5] W. Hulsbergen,[31] T. Humair,[60] R. J. Hunter,[55] M. Hushchyn,[79] D. Hutchcroft,[59] D. Hynds,[31] P. Ibis,[14] M. Idzik,[34] P. Ilten,[52] A. Inglessi,[37] K. Ivshin,[37] R. Jacobsson,[47] S. Jakobsen,[47] E. Jans,[31] B. K. Jashal,[46] A. Jawahery,[65] V. Jevtic,[14] F. Jiang,[3] M. John,[62] D. Johnson,[47] C. R. Jones,[54] B. Jost,[47] N. Jurik,[62] S. Kandybei,[50] M. Karacson,[47] J. M. Kariuki,[53] N. Kazeev,[79] M. Kecke,[16] F. Keizer,[54,47] M. Kelsey,[67] M. Kenzie,[55] T. Ketel,[32] B. Khanji,[47] A. Kharisova,[80] K. E. Kim,[67] T. Kirn,[13] V. S. Kirsebom,[48] S. Klaver,[22] K. Klimaszewski,[35] S. Koliiev,[51] A. Kondybayeva,[78] A. Konoplyannikov,[38] P. Kopciewicz,[34] R. Kopecna,[16] P. Koppenburg,[31] M. Korolev,[39] I. Kostiuk,[31,51] O. Kot,[51] S. Kotriakhova,[37] L. Kravchuk,[40] R. D. Krawczyk,[47] M. Kreps,[55] F. Kress,[60] S. Kretzschmar,[13] P. Krokovny,[42,e] W. Krupa,[34] W. Krzemien,[35] W. Kucewicz,[33,p] M. Kucharczyk,[33] V. Kudryavtsev,[42,e] H. S. Kuindersma,[31] G. J. Kunde,[66] T. Kvaratskheliya,[38] D. Lacarrere,[47] G. Lafferty,[61] A. Lai,[26] D. Lancierini,[49] J. J. Lane,[61] G. Lanfranchi,[22] C. Langenbruch,[13] O. Lantwin,[49] T. Latham,[55] F. Lazzari,[28,q] R. Le Gac,[10] S. H. Lee,[81] R. Lefèvre,[9] A. Leflat,[39,47] O. Leroy,[10] T. Lesiak,[33] B. Leverington,[16] H. Li,[71] L. Li,[62] X. Li,[66] Y. Li,[6] Z. Li,[67] X. Liang,[67] T. Lin,[60] R. Lindner,[47] V. Lisovskyi,[14] G. Liu,[71] X. Liu,[3] D. Loh,[55] A. Loi,[26] J. Lomba Castro,[45] I. Longstaff,[58] J. H. Lopes,[2] G. Loustau,[49] G. H. Lovell,[54] Y. Lu,[6] D. Lucchesi,[27,r] M. Lucio Martinez,[31] Y. Luo,[3] A. Lupato,[27] E. Luppi,[20,f] O. Lupton,[55] A. Lusiani,[28,s] X. Lyu,[5] S. Maccolini,[19,c] F. Machefert,[11] F. Maciuc,[36] V. Macko,[48] P. Mackowiak,[14] S. Maddrell-Mander,[53] L. R. Madhan Mohan,[53] O. Maev,[37] A. Maevskiy,[79] D. Maisuzenko,[37] M. W. Majewski,[34] S. Malde,[62] B. Malecki,[47] A. Malinin,[77] T. Maltsev,[42,e] H. Malygina,[16] G. Manca,[26,l] G. Mancinelli,[10] R. Manera Escalero,[44] D. Manuzzi,[19,c] D. Marangotto,[25] J. Maratas,[9,t] J. F. Marchand,[8] U. Marconi,[19] S. Mariani,[21,21,47] C. Marin Benito,[11] M. Marinangeli,[48] P. Marino,[48] J. Marks,[16] P. J. Marshall,[59] G. Martellotti,[30] L. Martinazzoli,[47] M. Martinelli,[24,g]

D. Martinez Santos,[45] F. Martinez Vidal,[46] A. Massafferri,[1] M. Materok,[13] R. Matev,[47] A. Mathad,[49] Z. Mathe,[47] V. Matiunin,[38] C. Matteuzzi,[24] K. R. Mattioli,[81] A. Mauri,[49] E. Maurice,[11,a] M. McCann,[60] L. Mcconnell,[17] A. McNab,[61] R. McNulty,[17] J. V. Mead,[59] B. Meadows,[64] C. Meaux,[10] G. Meier,[14] N. Meinert,[74] D. Melnychuk,[35] S. Meloni,[24,g] M. Merk,[31] A. Merli,[25] M. Mikhasenko,[47] D. A. Milanes,[73] E. Millard,[55] M.-N. Minard,[8] O. Mineev,[38] L. Minzoni,[20] S. E. Mitchell,[57] B. Mitreska,[61] D. S. Mitzel,[47] A. Mödden,[14] A. Mogini,[12] R. D. Moise,[60] T. Mombächer,[14] I. A. Monroy,[73] S. Monteil,[9] M. Morandin,[27] G. Morello,[22] M. J. Morello,[28,s] J. Moron,[34] A. B. Morris,[10] A. G. Morris,[55] R. Mountain,[67] H. Mu,[3] F. Muheim,[57] M. Mukherjee,[7] M. Mulder,[47] D. Müller,[47] K. Müller,[49] C. H. Murphy,[62] D. Murray,[61] P. Muzzetto,[26] P. Naik,[53] T. Nakada,[48] R. Nandakumar,[56] T. Nanut,[48] I. Nasteva,[2] M. Needham,[57] N. Neri,[25,n] S. Neubert,[16] N. Neufeld,[47] R. Newcombe,[60] T. D. Nguyen,[48] C. Nguyen-Mau,[48,u] E. M. Niel,[11] S. Nieswand,[13] N. Nikitin,[39] N. S. Nolte,[47] C. Nunez,[81] A. Oblakowska-Mucha,[34] V. Obraztsov,[43] S. Ogilvy,[58] D. P. O'Hanlon,[53] R. Oldeman,[26,l] C. J. G. Onderwater,[75] J. D. Osborn,[81] A. Ossowska,[33] J. M. Otalora Goicochea,[2] T. Ovsiannikova,[38] P. Owen,[49] A. Oyanguren,[46] P. R. Pais,[48] T. Pajero,[28,28,47,s] A. Palano,[18] M. Palutan,[22] G. Panshin,[80] A. Papanestis,[56] M. Pappagallo,[57] L. L. Pappalardo,[20] C. Pappenheimer,[64] W. Parker,[65] C. Parkes,[61] G. Passaleva,[21,47] A. Pastore,[18] M. Patel,[60] C. Patrignani,[19,c] A. Pearce,[47] A. Pellegrino,[31] M. Pepe Altarelli,[47] S. Perazzini,[19] D. Pereima,[38] P. Perret,[9] L. Pescatore,[48] K. Petridis,[53] A. Petrolini,[23,b] A. Petrov,[77] S. Petrucci,[57] M. Petruzzo,[25,n] B. Pietrzyk,[8] G. Pietrzyk,[48] M. Pili,[62] D. Pinci,[30] J. Pinzino,[47] F. Pisani,[19] A. Piucci,[16] V. Placinta,[36] S. Playfer,[57] J. Plews,[52] M. Plo Casasus,[45] F. Polci,[12] M. Poli Lener,[22] M. Poliakova,[67] A. Poluektov,[10] N. Polukhina,[78,v] I. Polyakov,[67] E. Polycarpo,[2] G. J. Pomery,[53] S. Ponce,[47] A. Popov,[43] D. Popov,[52] S. Poslavskii,[43] K. Prasanth,[33] L. Promberger,[47] C. Prouve,[45] V. Pugatch,[51] A. Puig Navarro,[49] H. Pullen,[62] G. Punzi,[28,i] W. Qian,[5] J. Qin,[5] R. Quagliani,[12] B. Quintana,[8] N. V. Raab,[17] R. I. Rabadan Trejo,[10] B. Rachwal,[34] J. H. Rademacker,[53] M. Rama,[28] M. Ramos Pernas,[45] M. S. Rangel,[2] F. Ratnikov,[41,79] G. Raven,[32] M. Reboud,[8] F. Redi,[48] F. Reiss,[12] C. Remon Alepuz,[46] Z. Ren,[3] V. Renaudin,[62] S. Ricciardi,[56] D. S. Richards,[56] S. Richards,[53] K. Rinnert,[59] P. Robbe,[11] A. Robert,[12] A. B. Rodrigues,[48] E. Rodrigues,[59] J. A. Rodriguez Lopez,[73] M. Roehrken,[47] A. Rollings,[62] V. Romanovskiy,[43] M. Romero Lamas,[45] A. Romero Vidal,[45] J. D. Roth,[81] M. Rotondo,[22] M. S. Rudolph,[67] T. Ruf,[47] J. Ruiz Vidal,[46] A. Ryzhikov,[79] J. Ryzka,[34] J. J. Saborido Silva,[45] N. Sagidova,[37] N. Sahoo,[55] B. Saitta,[26,l] C. Sanchez Gras,[31] C. Sanchez Mayordomo,[46] R. Santacesaria,[30] C. Santamarina Rios,[45] M. Santimaria,[22] E. Santovetti,[29,w] G. Sarpis,[61] M. Sarpis,[16] A. Sarti,[30] C. Satriano,[30,x] A. Satta,[29] M. Saur,[5] D. Savrina,[38,39] L. G. Scantlebury Smead,[62] S. Schael,[13] M. Schellenberg,[14] M. Schiller,[58] H. Schindler,[47] M. Schmelling,[15] T. Schmelzer,[14] B. Schmidt,[47] O. Schneider,[48] A. Schopper,[47] H. F. Schreiner,[64] M. Schubiger,[31] S. Schulte,[48] M. H. Schune,[11] R. Schwemmer,[47] B. Sciascia,[22] A. Sciubba,[22] S. Sellam,[68] A. Semennikov,[38] A. Sergi,[52,47] N. Serra,[49] J. Serrano,[10] L. Sestini,[27] A. Seuthe,[14] P. Seyfert,[47] D. M. Shangase,[81] M. Shapkin,[43] L. Shchutska,[48] T. Shears,[59] L. Shekhtman,[42,e] V. Shevchenko,[77] E. Shmanin,[78] J. D. Shupperd,[67] B. G. Siddi,[20] R. Silva Coutinho,[49] L. Silva de Oliveira,[2] G. Simi,[27,r] S. Simone,[18,k] I. Skiba,[20] N. Skidmore,[16] T. Skwarnicki,[67] M. W. Slater,[52] J. G. Smeaton,[54] A. Smetkina,[38] E. Smith,[13] I. T. Smith,[57] M. Smith,[60] A. Snoch,[31] M. Soares,[19] L. Soares Lavra,[9] M. D. Sokoloff,[64] F. J. P. Soler,[58] B. Souza De Paula,[2] B. Spaan,[14] E. Spadaro Norella,[25,n] P. Spradlin,[58] F. Stagni,[47] M. Stahl,[64] S. Stahl,[47] P. Stefko,[48] O. Steinkamp,[49,78] S. Stemmle,[16] O. Stenyakin,[43] M. Stepanova,[37] H. Stevens,[14] S. Stone,[67] S. Stracka,[28] M. E. Stramaglia,[48] M. Straticiuc,[36] S. Strokov,[80] J. Sun,[26] L. Sun,[72] Y. Sun,[65] P. Svihra,[61] K. Swientek,[34] A. Szabelski,[35] T. Szumlak,[34] M. Szymanski,[47] S. Taneja,[61] Z. Tang,[3] T. Tekampe,[14] F. Teubert,[47] E. Thomas,[47] K. A. Thomson,[59] M. J. Tilley,[60] V. Tisserand,[9] S. T'Jampens,[8] M. Tobin,[6] S. Tolk,[47] L. Tomassetti,[20,f] D. Torres Machado,[1] D. Y. Tou,[12] E. Tournefier,[8] M. Traill,[58] M. T. Tran,[48] E. Trifonova,[78] C. Trippl,[48] A. Tsaregorodtsev,[10] G. Tuci,[28,i] A. Tully,[48] N. Tuning,[31] A. Ukleja,[35] A. Usachov,[31] A. Ustyuzhanin,[41,79] U. Uwer,[16] A. Vagner,[80] V. Vagnoni,[19] A. Valassi,[47] G. Valenti,[19] M. van Beuzekom,[31] H. Van Hecke,[66] E. van Herwijnen,[47] C. B. Van Hulse,[17] M. van Veghel,[75] R. Vazquez Gomez,[44] P. Vazquez Regueiro,[45] C. Vázquez Sierra,[31] S. Vecchi,[20] J. J. Velthuis,[53] M. Veltri,[21,y] A. Venkateswaran,[67] M. Veronesi,[31] M. Vesterinen,[55] J. V. Viana Barbosa,[47] D. Vieira,[64] M. Vieites Diaz,[48] H. Viemann,[74] X. Vilasis-Cardona,[44,h] G. Vitali,[28] A. Vitkovskiy,[31] A. Vollhardt,[49] D. Vom Bruch,[12] A. Vorobyev,[37] V. Vorobyev,[42,e] N. Voropaev,[37] R. Waldi,[74] J. Walsh,[28] J. Wang,[3] J. Wang,[72] J. Wang,[6] M. Wang,[3] Y. Wang,[7] Z. Wang,[49] D. R. Ward,[54] H. M. Wark,[59] N. K. Watson,[52] D. Websdale,[60] A. Weiden,[49] C. Weisser,[63] B. D. C. Westhenry,[53] D. J. White,[61] M. Whitehead,[13] D. Wiedner,[14] G. Wilkinson,[62] M. Wilkinson,[67] I. Williams,[54] M. Williams,[63] M. R. J. Williams,[61] T. Williams,[52] F. F. Wilson,[56] W. Wislicki,[35] M. Witek,[33] L. Witola,[16] G. Wormser,[11] S. A. Wotton,[54] H. Wu,[67] K. Wyllie,[47] Z. Xiang,[5] D. Xiao,[7] Y. Xie,[7] H. Xing,[71] A. Xu,[4] J. Xu,[5] L. Xu,[3] M. Xu,[7] Q. Xu,[5] Z. Xu,[4] Z. Yang,[3]

Z. Yang,[65] Y. Yao,[67] L. E. Yeomans,[59] H. Yin,[7] J. Yu,[7] X. Yuan,[67] O. Yushchenko,[43] K. A. Zarebski,[52] M. Zavertyaev,[15,v] M. Zdybal,[33] M. Zeng,[3] D. Zhang,[7] L. Zhang,[3] S. Zhang,[4] W. C. Zhang,[3,z] Y. Zhang,[47] A. Zhelezov,[16] Y. Zheng,[5] X. Zhou,[5] Y. Zhou,[5] X. Zhu,[3] V. Zhukov,[13,39] J. B. Zonneveld,[57] and S. Zucchelli[19,c]

(LHCb Collaboration)

[1]*Centro Brasileiro de Pesquisas Físicas (CBPF), Rio de Janeiro, Brazil*
[2]*Universidade Federal do Rio de Janeiro (UFRJ), Rio de Janeiro, Brazil*
[3]*Center for High Energy Physics, Tsinghua University, Beijing, China*
[4]*School of Physics State Key Laboratory of Nuclear Physics and Technology, Peking University, Beijing, China*
[5]*University of Chinese Academy of Sciences, Beijing, China*
[6]*Institute of High Energy Physics (IHEP), Beijing, China*
[7]*Institute of Particle Physics, Central China Normal University, Wuhan, Hubei, China*
[8]*Universite Grenoble Alpes, Universite Savoie Mont Blanc, CNRS, IN2P3-LAPP, Annecy, France*
[9]*Université Clermont Auvergne, CNRS/IN2P3, LPC, Clermont-Ferrand, France*
[10]*Aix Marseille Universite, CNRS/IN2P3, CPPM, Marseille, France*
[11]*Université Paris-Saclay, CNRS/IN2P3, IJCLab, 91405 Orsay, France, Orsay, France*
[12]*LPNHE, Sorbonne Université, Paris Diderot Sorbonne Paris Cité, CNRS/IN2P3, Paris, France*
[13]*I. Physikalisches Institut, RWTH Aachen University, Aachen, Germany*
[14]*Fakultät Physik, Technische Universität Dortmund, Dortmund, Germany*
[15]*Max-Planck-Institut für Kernphysik (MPIK), Heidelberg, Germany*
[16]*Physikalisches Institut, Ruprecht-Karls-Universität Heidelberg, Heidelberg, Germany*
[17]*School of Physics, University College Dublin, Dublin, Ireland*
[18]*INFN Sezione di Bari, Bari, Italy*
[19]*INFN Sezione di Bologna, Bologna, Italy*
[20]*INFN Sezione di Ferrara, Ferrara, Italy*
[21]*INFN Sezione di Firenze, Firenze, Italy*
[22]*INFN Laboratori Nazionali di Frascati, Frascati, Italy*
[23]*INFN Sezione di Genova, Genova, Italy*
[24]*INFN Sezione di Milano-Bicocca, Milano, Italy*
[25]*INFN Sezione di Milano, Milano, Italy*
[26]*INFN Sezione di Cagliari, Monserrato, Italy*
[27]*INFN Sezione di Padova, Padova, Italy*
[28]*INFN Sezione di Pisa, Pisa, Italy*
[29]*INFN Sezione di Roma Tor Vergata, Roma, Italy*
[30]*INFN Sezione di Roma La Sapienza, Roma, Italy*
[31]*Nikhef National Institute for Subatomic Physics, Amsterdam, Netherlands*
[32]*Nikhef National Institute for Subatomic Physics and VU University Amsterdam, Amsterdam, Netherlands*
[33]*Henryk Niewodniczanski Institute of Nuclear Physics Polish Academy of Sciences, Kraków, Poland*
[34]*AGH—University of Science and Technology, Faculty of Physics and Applied Computer Science, Kraków, Poland*
[35]*National Center for Nuclear Research (NCBJ), Warsaw, Poland*
[36]*Horia Hulubei National Institute of Physics and Nuclear Engineering, Bucharest-Magurele, Romania*
[37]*Petersburg Nuclear Physics Institute NRC Kurchatov Institute (PNPI NRC KI), Gatchina, Russia*
[38]*Institute of Theoretical and Experimental Physics NRC Kurchatov Institute (ITEP NRC KI), Moscow, Russia*
[39]*Institute of Nuclear Physics, Moscow State University (SINP MSU), Moscow, Russia*
[40]*Institute for Nuclear Research of the Russian Academy of Sciences (INR RAS), Moscow, Russia*
[41]*Yandex School of Data Analysis, Moscow, Russia*
[42]*Budker Institute of Nuclear Physics (SB RAS), Novosibirsk, Russia*
[43]*Institute for High Energy Physics NRC Kurchatov Institute (IHEP NRC KI), Protvino, Russia*
[44]*ICCUB, Universitat de Barcelona, Barcelona, Spain*
[45]*Instituto Galego de Física de Altas Enerxías (IGFAE), Universidade de Santiago de Compostela, Santiago de Compostela, Spain*
[46]*Instituto de Fisica Corpuscular, Centro Mixto Universidad de Valencia—CSIC, Valencia, Spain*
[47]*European Organization for Nuclear Research (CERN), Geneva, Switzerland*
[48]*Institute of Physics, Ecole Polytechnique Fédérale de Lausanne (EPFL), Lausanne, Switzerland*
[49]*Physik-Institut, Universität Zürich, Zürich, Switzerland*
[50]*NSC Kharkiv Institute of Physics and Technology (NSC KIPT), Kharkiv, Ukraine*
[51]*Institute for Nuclear Research of the National Academy of Sciences (KINR), Kyiv, Ukraine*
[52]*University of Birmingham, Birmingham, United Kingdom*

[53]H.H. Wills Physics Laboratory, University of Bristol, Bristol, United Kingdom
[54]Cavendish Laboratory, University of Cambridge, Cambridge, United Kingdom
[55]Department of Physics, University of Warwick, Coventry, United Kingdom
[56]STFC Rutherford Appleton Laboratory, Didcot, United Kingdom
[57]School of Physics and Astronomy, University of Edinburgh, Edinburgh, United Kingdom
[58]School of Physics and Astronomy, University of Glasgow, Glasgow, United Kingdom
[59]Oliver Lodge Laboratory, University of Liverpool, Liverpool, United Kingdom
[60]Imperial College London, London, United Kingdom
[61]Department of Physics and Astronomy, University of Manchester, Manchester, United Kingdom
[62]Department of Physics, University of Oxford, Oxford, United Kingdom
[63]Massachusetts Institute of Technology, Cambridge, Massachusetts, USA
[64]University of Cincinnati, Cincinnati, Ohio, USA
[65]University of Maryland, College Park, Maryland, USA
[66]Los Alamos National Laboratory (LANL), Los Alamos, USA
[67]Syracuse University, Syracuse, New York, USA
[68]Laboratory of Mathematical and Subatomic Physics, Constantine, Algeria
(associated Universidade Federal do Rio de Janeiro (UFRJ), Rio de Janeiro, Brazil)
[69]School of Physics and Astronomy, Monash University, Melbourne, Australia
(associated Department of Physics, University of Warwick, Coventry, United Kingdom)
[70]Pontifícia Universidade Católica do Rio de Janeiro (PUC-Rio), Rio de Janeiro, Brazil
(associated Universidade Federal do Rio de Janeiro (UFRJ), Rio de Janeiro, Brazil)
[71]Guangdong Provencial Key Laboratory of Nuclear Science, Institute of Quantum Matter,
South China Normal University, Guangzhou, China
(associated Center for High Energy Physics, Tsinghua University, Beijing, China)
[72]School of Physics and Technology, Wuhan University, Wuhan, China
(associated Center for High Energy Physics, Tsinghua University, Beijing, China)
[73]Departamento de Fisica, Universidad Nacional de Colombia, Bogota, Colombia
(associated with I. Physikalisches Institut, RWTH Aachen University, Aachen, Germany)
[74]Institut für Physik, Universität Rostock, Rostock, Germany
(associated Physikalisches Institut, Ruprecht-Karls-Universität Heidelberg, Heidelberg, Germany)
[75]Van Swinderen Institute, University of Groningen, Groningen, Netherlands
(associated Nikhef National Institute for Subatomic Physics, Amsterdam, Netherlands)
[76]Universiteit Maastricht, Maastricht, Netherlands
(associated Nikhef National Institute for Subatomic Physics, Amsterdam, Netherlands)
[77]National Research Centre Kurchatov Institute, Moscow, Russia
(associated Institute of Theoretical and Experimental Physics NRC Kurchatov Institute (ITEP NRC KI), Moscow, Russia)
[78]National University of Science and Technology "MISIS", Moscow, Russia
(associated Institute of Theoretical and Experimental Physics NRC Kurchatov Institute (ITEP NRC KI), Moscow, Russia)
[79]National Research University Higher School of Economics, Moscow, Russia
(associated Yandex School of Data Analysis, Moscow, Russia)
[80]National Research Tomsk Polytechnic University, Tomsk, Russia
(associated Institute of Theoretical and Experimental Physics NRC Kurchatov Institute (ITEP NRC KI), Moscow, Russia)
[81]University of Michigan, Ann Arbor, Michigan, USA
(associated Syracuse University, Syracuse, New York, USA)

[a]Also at Laboratoire Leprince-Ringuet, Palaiseau, France.
[b]Also at Università di Genova, Genova, Italy.
[c]Also at Università di Bologna, Bologna, Italy.
[d]Also at Università di Modena e Reggio Emilia, Modena, Italy.
[e]Also at Novosibirsk State University, Novosibirsk, Russia.
[f]Also at Università di Ferrara, Ferrara, Italy.
[g]Also at Università di Milano Bicocca, Milano, Italy.
[h]Also at DS4DS, La Salle, Universitat Ramon Llull, Barcelona, Spain.
[i]Also at Università di Pisa, Pisa, Italy.
[j]Also at Universidad Nacional Autonoma de Honduras, Tegucigalpa, Honduras.
[k]Also at Università di Bari, Bari, Italy.
[l]Also at Università di Cagliari, Cagliari, Italy.
[m]Also at INFN Sezione di Trieste, Trieste, Italy.
[n]Also at Università degli Studi di Milano, Milano, Italy.
[o]Also at Universidade Federal do Triângulo Mineiro (UFTM), Uberaba-MG, Brazil.

[p]Also at AGH—University of Science and Technology, Faculty of Computer Science, Electronics and Telecommunications, Kraków, Poland.
[q]Also at Università di Siena, Siena, Italy.
[r]Also at Università di Padova, Padova, Italy.
[s]Also at Scuola Normale Superiore, Pisa, Italy.
[t]Also at MSU—Iligan Institute of Technology (MSU-IIT), Iligan, Philippines.
[u]Also at Hanoi University of Science, Hanoi, Vietnam.
[v]Also at P.N. Lebedev Physical Institute, Russian Academy of Science (LPI RAS), Moscow, Russia.
[w]Also at Università di Roma Tor Vergata, Roma, Italy.
[x]Also at Università della Basilicata, Potenza, Italy.
[y]Also at Università di Urbino, Urbino, Italy.
[z]Also at School of Physics and Information Technology, Shaanxi Normal University (SNNU), Xi'an, China.